Tellus (1980), *32*, 131–142

Some studies on moisture conditions in the Southern Hemisphere

By Y. VISWANADHAM, N. JAGAN MOHANA RAO[1] and G. S. S. NUNES[2], *Instituto de Pesquisas Espaciais, Conselho Nacional de Desenvolvimento Científico e Tecnológico, São José dos Campos, São Paulo, Brazil*

(Manuscript received January 19; in final form August 21, 1979)

ABSTRACT

Vertical cross-sections of the seasonal mean atmospheric humidity conditions on a planetary scale for the Southern Hemisphere are presented. The fields of mean precipitable water content are analysed for the four seasons of the year. Zonally averaged values of the various quantities at several levels are presented and compared, wherever possible, with previous results. The structure of these fields in association with general circulation patterns of the atmosphere is discussed. Precipitation efficiencies for the three continents, South America, Africa and Australia are estimated. Vertical cross-sections of atmospheric cooling rates for January and July are presented.

1. Introduction

Knowledge of total moisture present in the atmosphere is necessary for many purposes. Because of the growing need and current interest, more detailed information regarding the distribution of water vapour present at any moment in different air layers of the atmosphere is of fundamental importance in meteorological, hydrometeorological and electromagnetic wave propagation studies (Reber and Swope, 1972). Younkin et al. (1956) and Lowry (1972) pointed out the importance of vertically integrated moisture in the objective prediction of clouds and precipitation. A considerable number of investigations about atmospheric water vapour on a broad spectrum of scales has been made in the past. On a regional basis, the water vapour content over North America was studied by Benton and Estoque (1954) and Rasmusson (1967) among others. Kirryeva et al. (1958) presented seasonal distribution of water vapour density with heights over the territory of the U.S.S.R. Similar studies have been made for southern England (Hutchings, 1957), Australia (Hutchings, 1961), Africa (Peixoto and Obasi, 1965), India (Ananthakrishnan et al., 1965; Viswanadham et al., 1970).

The important role of water vapour in the energetics of the general circulation of the atmosphere has been studied and discussed by Peixoto (1965) and Starr and Saltzman (1966). Telegadas and London (1954) presented, for winter and summer, relative humidity distributions for the period 1949–51 at 850, 700 and 500 mb surfaces for the Northern Hemisphere. Studies for the entire Northern Hemisphere were carried out by Starr and White (1955), Starr and Peixoto (1958, 1964), and Starr et al. (1958) for the year 1950 and by Peixoto and Crisi (1965) for the IGY period. Bannon and Steele (1960) provided world-wide charts of total water vapour content at 850, 700 and 500 mb surface. Reitan (1960a, b) presented charts of monthly average total water vapour content over the U.S.A. for the 11-year period 1946–1956. Starr et al. (1969) presented the total pole-to-pole moisture conditions on a planetary scale during the IGY covering the calendar year 1958.

[1] Instituto de Planejamento e Estudos Ambientais, Universidade Estadual Paulista "Julio de Mesquita Filho", Campus de Presidente Prudente, São Paulo, Brazil.

[2] Fundação Centro Tecnológico de Minas Gerais, Belo Horizonte, Minas Gerais, Brazil.

0040-2826/80/020131-12$02.50/0

The present work provides a systematic study of the seasonal humidity conditions for the entire Southern Hemisphere. Due to lack of data, the study has been restricted to midseason months representing the four seasons of the year. However, the relationship obtained for the four seasons will be of value not only in future studies of large-scale atmospheric processes, but also in the preparation of climatic normals of water vapour content for the Southern Hemisphere.

2. Data source and representativeness

The present study is based on the data given in Cimate of Upper Air-Southern Hemisphere (Taljaard et al., 1969). The grid point data of mean ambient and dew-point temperatures from surface to 500 mb level for every 5° longitude around each 5° latitude circle between the equator and 90° S are utilized. The rainfall data for different stations, as given in the technical publication (WMO, 1967), are used in evaluating the precipitation efficiency values.

The most noticeable characteristic of the Southern Hemisphere is the large expanse of ocean with relatively few land masses. Any contemplated atmospheric study of the Southern Hemisphere is hindered by the shortage of observing stations and paucity of data. There are uncertainties inherent in the basic data and also portions of the computational procedures may introduce errors in the estimates of the variously derived fields. Some aspects of these problems have been discussed by Hutchings (1957) among others. Although they are very important sources of uncertainty in dealing with studies pertaining to restricted time and space, it seems safe to assume that for studies of a large scale and embracing long periods of time such as the present one, the accuracy of the data is sufficient to depict the main characteristics of the water vapour content in the atmosphere. By far the bulk of the water content of the atmosphere and most of its flux occur below 400 mb level where the upper air observation, as obtained by classical methods, is more abundant and the reliability of the instruments is greater. Thus it seems that vertical measurements in the lower atmosphere are fairly adequate for our present study. The approximations and the reliability of the individual parameters are discussed at length in the introductory pages by Taljaard et al. (1969).

The values of mixing-ratio r (g kg^{-1}) are computed from the grid point data at levels corresponding to the surface, 850, 700 and 500 mb levels. To simplify the computation, the specific humidity is replaced by the mixing-ratio. This would have the effect of slightly overestimating the total water vapour content; however, a partial compensation is conveniently obtained by setting the acceleration of gravity .equal to 10 m s^{-2}. Neither of these approximations introduces a significant error; furthermore since errors are consistent in sign, the total water vapour content will be unaffected.

3. Precipitable water

The precipitable water (PW) of a column of air is defined as the depth of water which would accumulate if all the water vapour in that column were precipitated. The total mass of vapour in a small element of humid air of 1 cm^2 cross-section and dh thickness is

$$\Delta M_v = q\rho_a\, dh \tag{1}$$

where ρ_a is the density of air, M_v is the mass of water vapour and q represents the specific humidity. Introducing the equation of hydrostatic equilibrium, it is found that the thickness of liquid water that would be precipitated is

$$W = \frac{1}{g}\int_{P_{h=0}}^{P_0} q\, dP \tag{2}$$

if the column extends from pressure P_0 to P_h (=0).

Further, it has been considered that for practical purposes q is equal to mixing-ratio (r) and the acceleration of gravity (g) is equal to 10 m s^{-2} and the PW present from the surface to 500 mb level may be considered as equal to the total amount of W, since the amount above that elevation is very small. The total mean precipitable water content for each grid point data is expressed by

$$W = \frac{1}{g}\int_{500}^{P_0} \bar{r}\, dP \tag{3}$$

where W will be given in g cm^{-2}. The meteorological parameters for each layer of the atmosphere are computed utilizing International Meteorological Tables (WMO, 1968). The total precipitable water is obtained from eq. (3).

4. Distribution of precipitable water

The distribution of mean precipitable water (*PW*) is presented for the four midseason months (Figs. 1–4). The analyses show a continuous decrease of *PW* from the equator to the pole, which is to be expected since the ability of the atmosphere to retain water vapour is a function of the temperature. The areas of largest *PW* on the maps (Figs. 1–4) are generally located, as would be expected, in tropical regions, because of the high dry-bulb and dew-point temperatures and also the large evaporation. The analysis shows the influence of oceans and continents on the distribution of the water vapour content in the atmosphere. On the whole, the amount of *PW* is higher over the oceans, with the exception of the Amazon basin, in general agreement with the results obtained by Bannon and Steele (1960) and Starr et al. (1969). There is another exceptional region in middle latitudes, southern Chile, where relatively warm air from the sea undergoes forced upward motion to a substantial height. Over high ground, total *PW* contents are no doubt smaller than over neighbouring lower lying areas but it was not practicable to make any adjustments for the effects of topography.

In marked contrast to the high *PW* regions are the dry polar regions, where the mixing-ratios are always very low because of the low temperatures and very limited evaporation. The dry areas in the

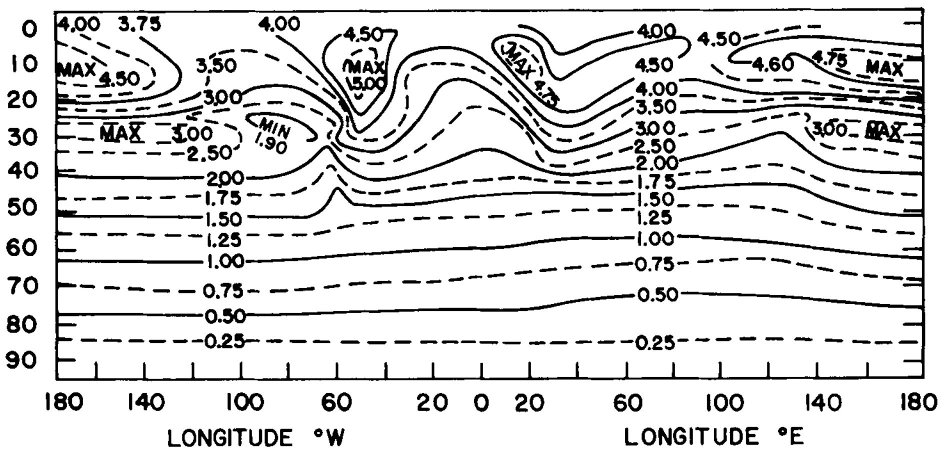

Fig. 1. Isolines of total precipitable water in g cm^{-2}—January.

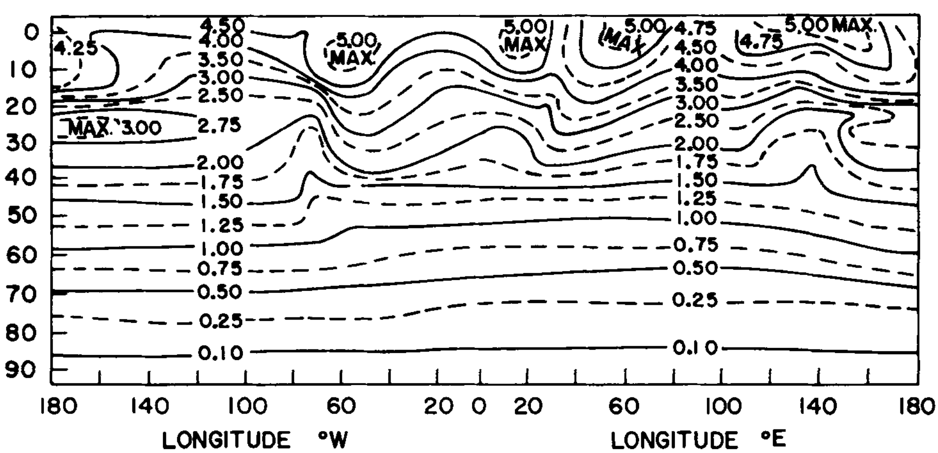

Fig. 2. Isolines of total precipitable water in g cm^{-2}—April.

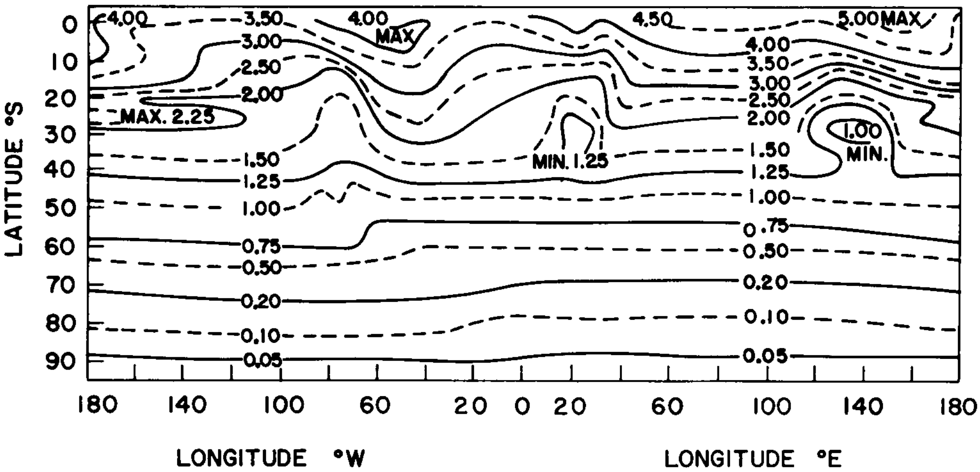

Fig. 3. Isolines of total precipitable water in g cm^{-2}—July.

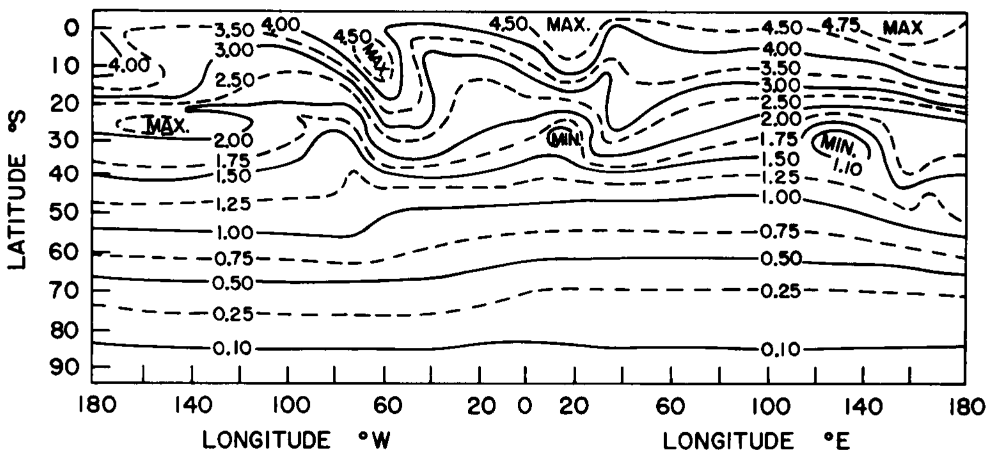

Fig. 4. Isolines of total precipitable water in g cm^{-2}—October.

subtropical region of the Pacific and Australia and the arid strips on the lee sides of southern America are easily noted. The observed low centre of *PW* over central Australia is similar to that found by Hutchings (1961).

A certain break of zonality in the variation of the isolines is observed over cool and warm ocean currents. With cold currents, the *PW* decreases. This occurs, for example, over the Peruvian Current and also the current caused by the westerlies near the southwestern coat of Australia. The warm currents are connected with an increase in the *PW* totals. Such an increase is observed over a branch of south equatorial Pacific Ocean current and over the warm currents in the Indian Ocean and the Atlantic Ocean. The maximum *PW* occurs over the warm equatorial currents with a frequent occurrence of clouds. The maximum in the *PW* is observed over the Pacific Ocean and equals 5 g cm^{-2}. In this connection it should be noted that the minimum *PW* values are related to desert (due to the high temperatures, low atmospheric moisture content and insignificant cloud). For example, a notable decrease of *PW* is observed over the Great Sandy and Victoria deserts of Australia, Kalahari Desert of South Africa and Patagonia and Atacama deserts of South America (Fig. 3). The effects of topography are also evident over the Andes, the highlands of Ethiopia and the mountains of Kenya.

Larger values of total PW occur in summer and lower values in winter. The PW appears to have influence on maritime climates (Viswanadham et al., 1970). Thus at coastal regions, there are characteristically larger values of PW. In the northern countries of South America the sharply contrasted dry and wet seasons are related to the regions of trade winds. In the dry season these winds sweep the entire region, while in the wet season, calm and variable winds prevail. In the basin of the Amazon River, these winds give the maximum amounts of PW where they ascend the Andean Slopes (Krueger, 1970).

The desert areas on the west coast of South America, extending from the equator southward to the latitude of Santiago, are due to a combination of the effects of the Andes and the cold Peruvian Current. The mean flow in this area, up to 500 mb, is generally from the east, which favours high moisture content and precipitation along the east slopes of the Andes and reduced moisture content on the west slopes. The sinking motion along the west slopes acts to stabilize the atmosphere in this region, thus producing conditions which are not favourable for convection. The cold oceanic waters also act to increase the stability. Therefore, the values of PW are generally low in this region. In southern Chile the summer and winter seasons are moderately wet. Condensation and precipitation of moisture occurs as the air ascends along the slopes of the Andes. By the time air passes the crest of the mountains, the moisture has been depleted by precipitation so that the winds on the leeward slopes are warm and dry. Therefore, the mountains can be looked upon as casting a "PW shadow" over southern Argentina.

Africa, like South America, lies largely within the tropics. Moreover, along the southern portion of the western coasts, the cool Benguela Current moves northward and on the eastern coast there are the warm tropical currents of the Indian Ocean, which create conditions closely parallel to those found around the South American Continent. The higher PW values are observed over sections of Ethiopia in January, April and October.

Because Australia is centred on the Southern Tropic, temperatures far below freezing are to be found only in a few areas of the continent, e.g. in the south at high elevations (in winter). In the arid interior, maximum temperatures are very high, ranking with those of the hottest regions of the earth. In the southern winter the high pressure crosses the interior of Australia, and all except the southernmost parts of the continent are dry. In summer, on the other hand, this pressure belt has moved south of the continent, still giving dry conditions over the southern and western areas.

Charts of PW for the autumn (April) and spring (October) seasons are shown in Figs. 2 and 4, respectively. The chart for spring shows basically a pattern similar to winter, whereas the chart for autumn shows the same pattern as for summer. Using the grid point values of total PW, an estimate of the meridional distribution of zonally averaged PW, $\bar{W}$, is obtained. The resulting values for the four midseason months and annual values are shown in Fig. 5. Sasamori et al. (1972) have also presented the PW in a vertical air column at each 10° S latitude belt. In Fig. 5 the curve with the results obtained by Sellers (1969) is included for comparison. Sellers' values are slightly higher and were obtained by independent means. But overall the agreement is good. As expected, the curves for $\bar{W}$ show maximum values at the equator and show continuous decrease from equator to the pole ($\partial\bar{W}/\partial\phi < 0$, where ϕ is latitude) with the steepest gradient over the subtropical latitudes. The grand average of PW is of the order of 2 g cm^{-2}. It is then clear that the storage of water vapour in the atmosphere is relatively small and the amount present could be completely removed by the average precipitation acting alone with a period of 10 days (Starr and Peixoto, 1964). However, the total water vapour content for the entire atmosphere is still comparable to the water content in the rivers of the earth, as estimated by hydrologists. The integrated total PW data given in this study can be used to locate the net inflow regions (convergence) or outflow regions (divergence) of water vapour for a particular area.

5. Precipitation efficiency

An idea of the latitudinal variation of the precipitation efficiency (PE) can be obtained by dividing the mean daily precipitation by the average precipitable water. It follows that the PE is given by

$$PE = \frac{MP}{ND \times PW} \times 100\% \tag{4}$$

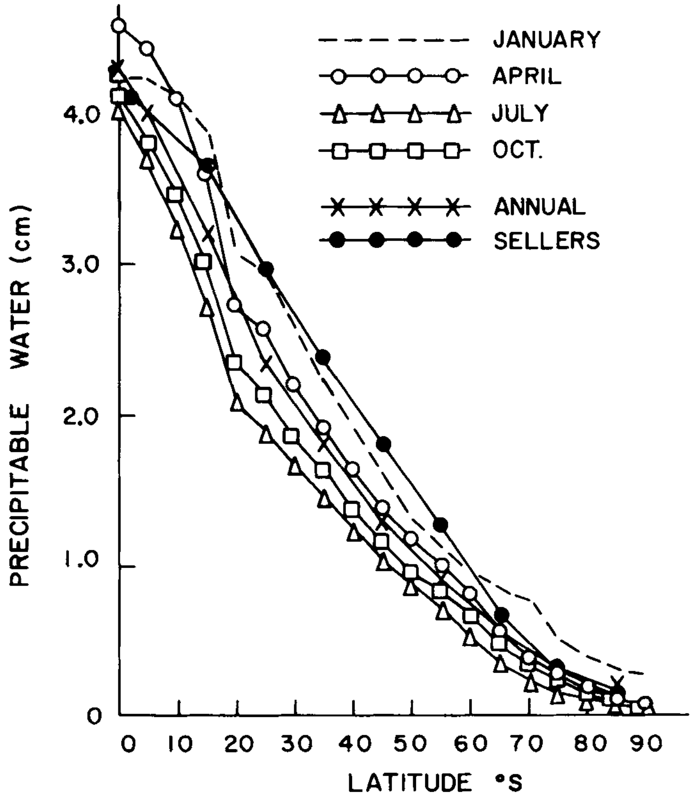

Fig. 5. The meridional distribution of zonally averaged precipitable water (g cm^{-2}) for different seasons.

where *MP* is mean monthly precipitation in mm, *PW* precipitable water in mm and *ND* number of days in a month. For convenience, this ratio can be thought of as the fraction of the average moisture overhead which falls as precipitation on an average day. The *PE* values are calculated for South America, Africa and Australia. They are presented in Figs. 6–11. In South America in January (Fig. 6), the *PE* is low on the west coast and high on the east coast. The *PE* is very low on the western side of the Andes and slightly higher on the eastern side, reflecting the orographic effect on precipitation. Maxima are located in the central Amazon, central tropical Brazil, east coast of Brazil (20° S) and over Uruguay. Maxima of July (Fig. 7) *PE* (20%) exist over the east coast of tropical Brazil (5–15° S, 35–40° W), central Amazon, southern Brazil (Rio Grande do Sul) and Uruguay. Lowest values, less than 1%, occur over the eastern region of central tropical Brazil (10° S, 45° W), the foothills of the Andes in Argentina, the

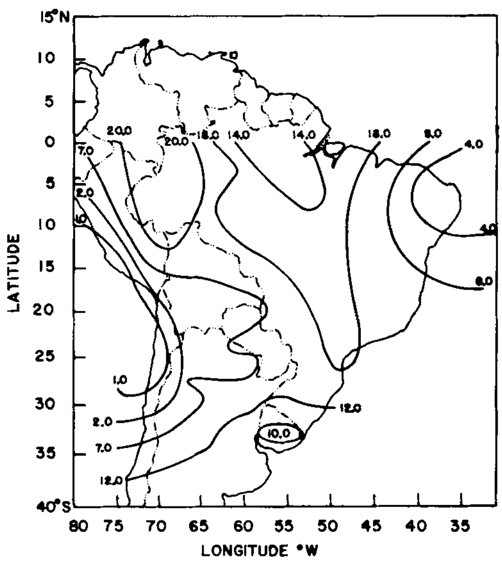

Fig. 6. Precipitation efficiency (%) in South America—January.

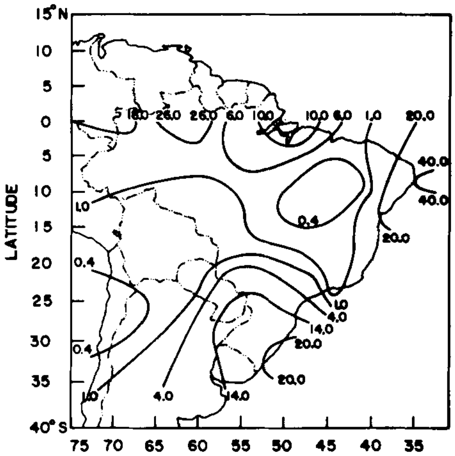

Fig. 7. Precipitation efficiency (%) in South America—July.

island of Pampa (13° 15′ S, 73°08′ W) and over Bolivia. Precipitation efficiencies are generally lower in July (Fig. 7) than in January. However, the lowest values occur during summer along the Pacific Coast, which is under the influence of the very stable Pacific high-pressure system. Values in excess of 10% are found only in the southern states of Brazil and along the northeastern border. Slightly higher values of maxima and lower values of minima are noticed in July than in January.

The *PE* values of Africa (Fig. 8) show that the high values occur over Gabon, Tanzania and south central regions and low values occur over the remaining areas. Below 32° S over Africa in July (Fig. 9), there are slightly higher values of *PE* (>10%) and the remaining regions are completely dry. However, the vast plateaus exert a profound effect on the climate of the eastern and southern portions in Africa. In January, pronounced heating produces a mean low pressure area south of the equator. This vast cyclone separates the well-developed oceanic subtropical anticyclones to the east and west (south of the equator 20° S to 35° S). The January upper air circulation is also probably weak, in view of the diffuse surface cyclone and the indeterminate temperature gradient. The mean July circulation is approximately the converse of the January pattern.

Figs. 10 and 11 show that the *PE* values of Australia are larger along the coastal areas of the country. In Fig. 11, the isolines are poorly presented due to lack of mean monthly precipitation data. On an average, lowest *PE* values appear to be found over the extensive area extending northwestward from Woomera and southwestward from Alice Springs. Maximum values are observed over the areas of the Gulf of Carpentaria, Cape York Peninsula and Townville in summer, whereas in winter they are noticed over New South Wales and Victoria. These general considerations demonstrate the importance of topography on the distribution of precipitation and temperature.

The prominent indentations of the Australian continent are the Gulf of Carpentaria and the Great Australian Bight. Since, north of 25° S, the pre-

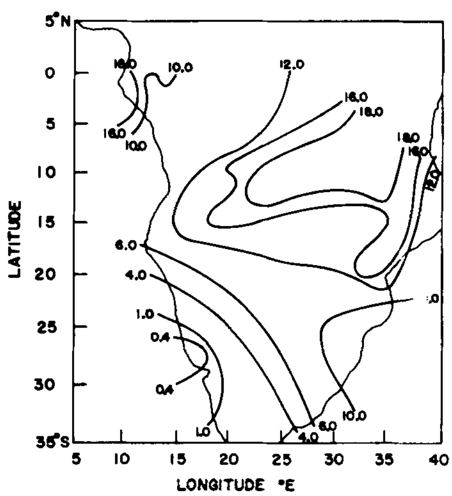

Fig. 8. Precipitation efficiency (%) in Africa—January.

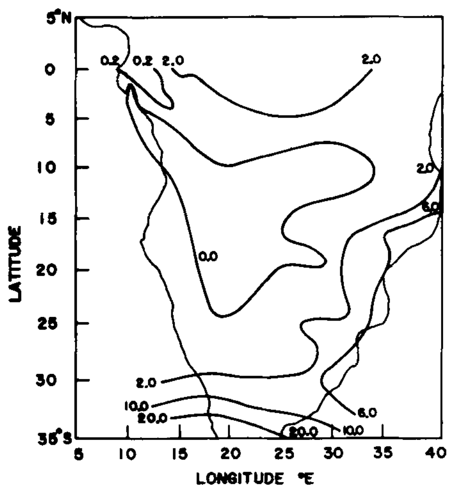

Fig. 9. Precipitation efficiency (%) in Africa—July.

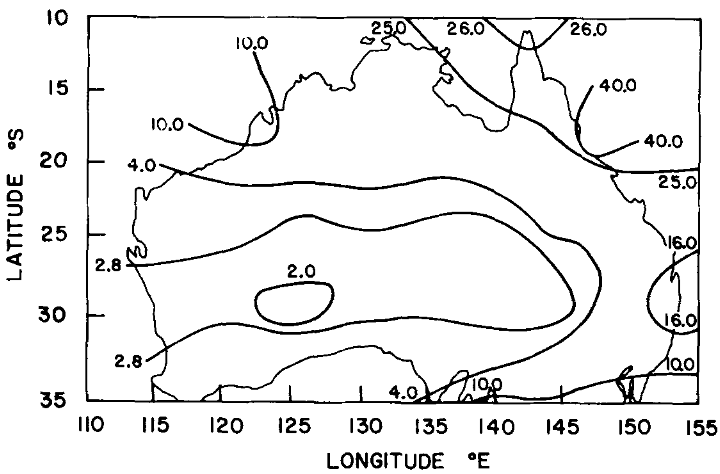

Fig. 10. Precipitation efficiency (%) in Australia—January.

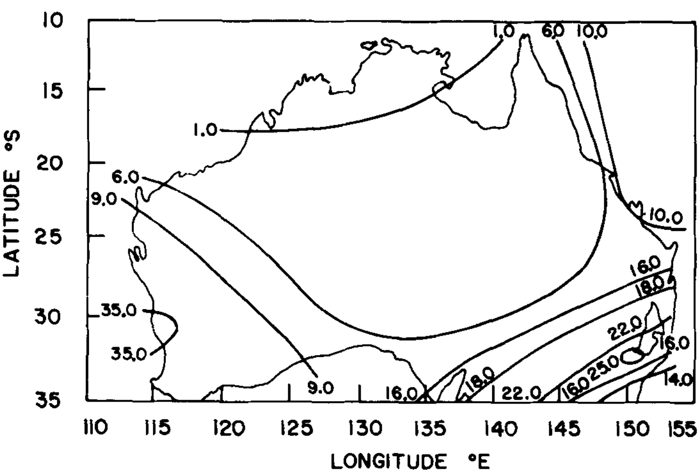

Fig. 11. Precipitation efficiency (%) in Australia—July.

vailing air flow is from east to west, orographical lifting results in considerably heavier precipitation along the east coast than over the central or western section of Australia. South of 30° S, the southeastern highlands also favour higher rainfall over Victoria and New South Wales than across the low-lying lands around the Great Australian Bight. Besides favouring orographic precipitation, the eastern highlands shelter the interior from direct invasions of maritime air, consequently, the dry air masses of central Australia are noticed during summer. In contrast to South America and other continents, the flat Australian continent does not offer any obstacle to the west–east circulation. The migratory anticyclonic centres rarely penetrate further north than 25 °S, and consequently the winter southeast trades and the cyclonic circulation in summer are reasonably constant across northern Australia. These indicate that the general climatological features in summer and winter clearly reflect the variability of *PE* values over Australia.

6. Atmospheric cooling rates

Some complexities in studies of atmospheric dynamics can be considerably simplified if suitable approximations are made in computations of radiative heating and cooling in the atmosphere. Radiative cooling in the troposphere, in the absence of clouds, depends largely on the vertical distribution of temperature and water vapour. Dickinson (1969), however, suggested that a good first approximation to the radiative cooling distribution would be a linear dependence on the local free-air temperature. The present study reports the results of some calculations of radiative flux divergence in the Southern Hemisphere to support this approximation. London and Sasamori (1970) studied the linear dependence of radiative cooling rate on the local mean free-air temperature in the model clear atmosphere for winter and summer seasons at latitudes 0°, 30° and 60° of the Northern and Southern Hemispheres. They obtained the following approximate least square equation:

$$C_R \sim 0.017T + 1.8 \quad (5)$$

where C_R is the cooling rate in °C per day and T is the mean free-air temperature in °C. The advantage of this equation depends on the specific problem to be studied.

The radiative cooling rates are calculated at four standard levels for the four midseason months using eq. (5) and mean free-air temperatures. The vertical distribution of zonally averaged values of cooling rates for January and July is shown in Figs. 12 and 13, respectively. The results for April and October show the same pattern as January and July, respectively, and are not presented. It is evident that they are not true representative values because the free-air temperatures are averaged values for clear and cloudy conditions. However, the results might be useful in the climatological heat budget along with the climatological characteristics of the net radiation and its components for the earth–atmosphere system. The seasonal range is very small and radiative cooling rates are slightly higher in summer (January) and lower in winter

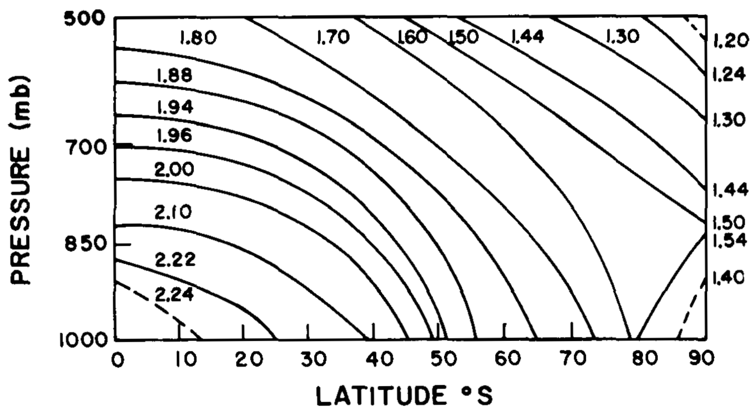

Fig. 12. Vertical distribution of zonally averaged values of the radiative cooling rates in °C per day—January.

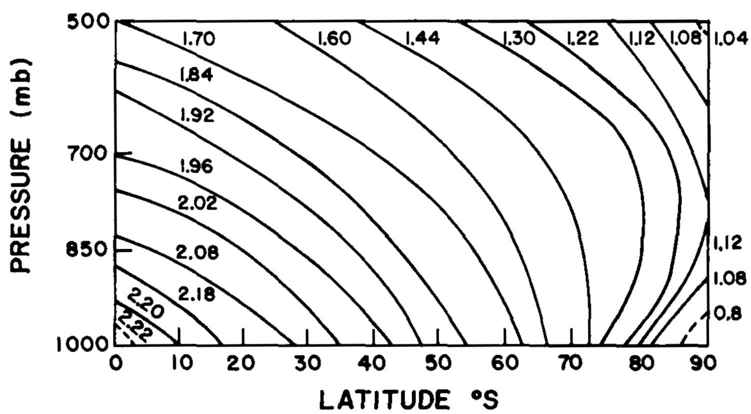

Fig. 13. Vertical distribution of zonally averaged values of the radiative cooling rates in °C per day—July.

(July). On the whole, they are a maximum in the low latitudes. The inhomogeneous distribution of radiative temperature changes is caused mainly by the lack of a uniform cloud cover. Minimum values of radiative temperature changes are observed in polar latitudes. The meridional gradient of radiative cooling in the troposphere shows that the cooling rates decrease southward.

Clouds play a dominant role in determining the radiative properties of the atmospheric layers above and below the middle level of about 500 mb (Cox, 1969). The maximum cooling of the lower layer is accomplished by having a cloud low in the layer. In reality, there would be a slight decrease in the cooling of the upper layer as the elevation of the cloud deck beneath is increased. A cloud high in the troposphere acts as a "lid" and does not allow the atmosphere to cool effectively. Dopplick (1972) has presented the latitude-height contours of total net radiative cooling rate for December–February and for June–August. It is obvious from the diagrams of Dopplick (1972) and our Figs. 12 and 13 that the cooling rates at a point bear some relation to the ambient temperature at that point. For instance, the troposphere has high cooling rates because of high temperature and high humidity, and the infrared cooling to space dominates the solar heating. These cooling rates are accentuated to a maximum just below the tropopause by the abundance of middle level cloud, which results from the adiabatic expansion occurring in the mean upward motion of the ascending branch of the Hadley cells. Clouds both increase the infrared loss and decrease the solar heating.

The mean meridional distribution of the total cloud cover is shown by van Loon (1972, his Fig. 6.3) for the months of January and July. In both seasons, a maximum cloud cover of 80–85% is found in the polar front region 60–70° S. The region of minimum clouds shifts southward from 15° S in winter to 30° S in summer. Hemispheric averages of the cloud cover are given by Sasamori et al. (1972, their Table 2.1). Total cloudiness is greater in the southern summer (58% in January) as compared to the southern winter (54% in July). Correspondingly, there are slightly large cooling rates during the summer than during the winter.

In Figs. 12 and 13, the cooling rates in the layer 1000 mb to 900 mb are lower than the cooling rates in the layer 900–500 mb at the polar latitudes (over 75 to 90° S). This is due to the rapid decrease of humidity with height in polar regions. The rapid decrease in humidity causes polar inversions which are generally noticed below 900 mb level. The minimum cooling rate occurs at the base of the inversions, while the maximum is near its upper boundary. In other words, a sudden decrease in specific humidity from the lower level to the one above causes very ineffective screening of the net upward flux. The result is maximum divergence leading to higher cooling rate over the inversion. The latitudinal gradient of cooling rate is larger in winter than in summer in the latitude belt 70–90° S, Sasamori et al. (1972) have also reported the same result from the numerical integration of radiative transfer equation. This latitudinal gradient of cooling rate contributes to the generation of mean zonal available potential energy that is used in driving the large-scale circulations in the Southern Hemisphere (Sasamori et al., 1972). The cooling rates presented in Figs. 12 and 13 are larger than those of Dopplick (1972). The high cooling rates near the tropical regions are due to the high temperatures and high humidities there and are, in fact, probably underestimated by Dopplick (1972). Recent works of Bignell (1970) and Platt (1972) have shown that infrared emission by water vapour in the atmospheric window itself is considerably enhanced at high relative humidity and becomes a very significant factor in tropical regions.

If mean values of the profiles are known, as they are for the grid point, a better estimate of the cooling rates could be obtained rather than using the regression results of London and Sasamori (1970), i.e. eq. (5). However, this would require values above the pressure level 500 mb. Our analysis shows that the regression equation (5) is quite adequate to study the climatological heat budget.

7. Concluding remarks

With the possible exception of a portion of the Antarctic region, it is felt that the present study reliably reflects humidity conditions over the Southern Hemisphere. It is hoped that these results will offer added insight into these conditions and will help to provide the basis for further intesive studies. The agreement of the results with those obtained by the other investigators for the Southern Hemisphere seems to confirm the consistency of the approach followed. The information presented in this study would be a useful supplement to regions where few or no balloon soundings are available. With an improvement of the Southern Hemisphere network and with information obtained by new instrumental techniques, much can be done to improve the actual results.

8. Acknowledgements

The authors are grateful to Dr Nelson de Jesus Parada, Director, and Dr Luiz Gylvan Meira Jr, Coordinator of the Department of Meteorology, Instituto de Pesquisas Espaciais, São José dos Campos, São Paulo, Brazil; the authorities of Instituto de Planejamento e Estudos Ambientais, Universidade Estadual Paulista, Presidente Prudente, São Paulo, Brazil, and Fundação Centro Tecnológico de Minas Gerias, Belo Horizonte, Minas Gerais, Brazil, for the encouragement. They are also grateful to Professor R. P. Kane and Dr Vernon E. Kousky for reading the manuscript. Thanks are also due to Miss Fátima Ricco dos Santos for typing the manuscript and Mr Carlos Roberto dos santos and his group members for drafting the figures. Finally, we are grateful to the referees for their useful comments. This work was partially supported by the Financiadora de Estudos e Projetos (FINEP) under contract B-28-79-001.

REFERENCES

Ananthakrishnan, R., Selvan, M. M. and Chellappa, R. 1965. Seasonal variation of precipitable water vapour in the atmosphere over India. *Ind. J. Meteor. Geophys. 16*, 371–384.

Bannon, J. K. and Steele, L. P. 1960. Average water vapour content of the air. Geophys. Mem., 13. London: Meteor. Office, 38 pp.

Benton, G. S. and Estoque, M. A. 1954. Water vapour transfer over the North American Continent. *J. Meteor. 11*, 462–477.

Bignell, M. J. 1970. The water vapour infra-red continuum. *Quart. J. Roy. Met. Soc. 96*, 390–403.

Cox, S. K. 1969. Radiation models of mid-latitude synoptic features. *Mon. Wea. Rev. 97*, 637–651.

Dickinson, R. E. 1969. Vertical propagation of planetary Rossby wave through an atmosphere with Newtonian cooling. *J. Geophys. Res. 74*, 929–938.

Dopplick, T. G. 1972. Radiative heating of the global atmosphere. *J. Atmos. Sci. 29*, 1298–1294.

Hutchings, J. W. 1957. Water vapour flux and flux divergence over southern England: summer 1954. *Quart. J. Roy. Met. Soc. 83*, 30–48.

Hutchings, J. W. 1961. Water vapour transfer over the Australian continent. *J. Meteor. 18*, 615–634.

Kirryeva, N. M., Kogan, S. Ya. and Ikuznetsova, M. A. 1958. Srednesezonnoe raspredelenie plotnosti vodianogo para po Vysote dlia territorii S.S.S.R. *Izv. Akad. Nauk. S.S.S.R., Ser. Geofiz. 5*, 669–672.

Krueger, A. F. 1970. The zontal variation of cloudiness and convection over the tropics. Proc. Symp. Trop. Meteorology, Hawaii, pp. 1–2.

London, J. and Sasamori, T. 1970. Radiative cooling as a function of temperature and water vapour in the free atmosphere. *J. Geophys. Res. 75*, 6862–6863.

Lowry, D. A. 1972. Climatological relationships among precipitable water, thickness and precipitation. *J. Appl. Meteor. 11*, 1326–1333.

Peixoto, J. P. 1965. On the role of water vapour in the energetics of the general circulation of the atmosphere. *Portugal Phys., Lisboa 4* (*2*), 135–170.

Peixoto, J. P. and Crisi, A. R. 1965. Hemispheric humidity conditions during the IGY. Sci. Report No. 6, Planetary Circulation Project, Mass. Inst. Tech., Cambridge, Mass.

Peixoto, J. P. and Obasi, G. O. P. 1965. Humidity conditions over Africa during the IGY. Sci. Report No. 7, Planetary Circulation Project, Mass. Inst. Tech., Cambridge, Mass.

Platt, C. M. R. 1972. Airborne infra-red radiance measurements (10–12 micron wavelength) off tropical east coast Australia. *J. Geophys. Res. 77*, 1597–1609.

Rasmusson, E. M. 1967. Atmospheric water vapour transport and water balance of North America. *Mon. Wea. Rev. 95*, 403–426.

Reber, E. E. & Swope, J. R. 1972. On the correlation of total precipitable water in a vertical column and absolute humidity at the surface. *J. Appl. Meteor. 11*, 1322–1325.

Reitan, C. H. 1960a. Distribution of precipitable water vapour over the continent United States. *Bull. Am. Meteor. Soc. 41*, 79–87.

Reitan, C. H. 1960b. Mean monthly values of precipitable water over United States, 1946–1956. *Mon. Wea. Rev. 88*, 25–35.

Sasamori, T., London, J. and Hoyt, D. V. 1972. Radiation budget of the Southern Hemisphere. *Meteorol. Monographs 13* (*35*). Boston: Am. Meteor. Soc., 9–23.

Sellers, W. D. 1969. *Physical climatology*. Chicago: The University of Chicago Press.

Starr, V. P. and Peixoto, J. P. 1958. On the global balance of water vapour and the hydrology of deserts. *Tellus 10*, 189–194.

Starr, V. P., Peixoto, J. P. and Livadas, G. C. 1958. On the meridional flux of water vapour in the Northern Hemisphere. *Geof. Pura Appl. 39*, 174–185.

Starr, V. P. and Peixoto, J. P. 1963. The hemispheric eddy flux of water vapour and its implications for the mechanics of the general circulation. *Arch. f. Met. Geoph. U. Biokl. A14*, 111–130.

Starr, V. P., Peixoto, J. P. and McKean, R. G. 1969. Pole-to-pole moisture conditions for the IGY. *Pure and Appl. Geophys. 75*, 1969/IV, 300–331.

Starr, V. P. and Saltzman, B. 1966. Observational studies of the atmospheric general circulation. Mass. Inst. Tech., Dept. Meteor., Cambridge, Mass., Planetary Circulation Project Sci. Report No. 2, 473–591.

Starr, V. P. and White, R. M. 1955. Direct measurement of the hemispheric poleward flux of water vapour. *J. Mar. Res. 14*, 217–225.

Taljaard, J. J., van Loon, H., Crutcher, H. L. and Jenne, R. L. 1969. Cimate of upper air, Part I—Southern Hemisphere, vol. I—Temperature, dew-point and heights at selected pressure levels. NAVAIR 50-1C-55. A joint production of NCAR, ESSA-NWRC and DOD., Washington, D.C.

Telegadas, K. and London, J. 1954. A physical model of the Northern Hemisphere troposphere for winter and summer. New York University, Sci. Report, No. 1, contract AF19 (122)—165, 55 pp.

van Loon, H. 1972. Cloudiness and precipitation. *Meteorol. Monogr. 13* (*35*). Boston: Am. Meteor. Soc., 101–111.

Viswanadham, Y., Ramanadham, R. and Sri Rama Krishna, Y. 1970. Studies on precipitable water over tropical stations in relation to monsoon flow. *Pure and Appl. Geophys. 79*, 1970/II, 103–119.

World Meteorological Organization 1967. Climatological Normals (CLINO) for climate and climate ship stations for the period 1931–1960. WMO-117-TP. 52. Geneva: WMO.

World Meteorological Organization 1968. International Meteorological Tables. WMO-NO-188-TP.94. Geneva: WMO.

Younkin, R. J., LaRue, J. A. and Sanders, F. 1965. The objective prediction of cloud and precipitation using vertically integrated moisture and adiabatic vertical motions. *J. Appl. Meteorol. 4*, 3–17.

НЕКОТОРЫЕ ИССЛЕДОВАНИЯ УСЛОВИЙ УВЛАЖНЕНИЯ В ЮЖНОМ ПОЛУШАРИИ

Для Южного полушария в планетарном масштабе представлены вертикальные разрезы средних сезонных условий увлажнения. Для четырех сезонов года анализируются поля среднего содержания выпадающей влаги. Зонально осредненные значения различных величин на разных уровнях представлены и сравнены, где это возможно, с предыдущими результатами. Обсуждается структура этих полей в связи с особенностями общей циркуляции атмосферы. Оценены эффективности осадков для терх континентов — Южной Америки, Африки и Австралии. Представлены вертикальные разрезы скоростей охлаждения атмосферы для января и июля.